

## Melting and magnetic ordering in transition-metal microclusters

H. T. Diep\* and S. Sawada

*Fundamental Research Laboratories, NEC Corporation, 4-1-1 Miyazaki, Miyamae-ku, Kawasaki 213, Japan*

S. Sugano

*Institute for Solid State Physics, University of Tokyo, Roppongi, Minato-ku, Tokyo 106, Japan*

(Received 16 November 1988)

Melting behavior of transition-metal clusters is studied by extensive Monte Carlo simulation for cluster sizes from  $N=7$  to 17 atoms. Physical quantities such as internal energy, specific heat, bond-length average, and bond-length fluctuations are shown. A long-range magnetic interaction between spins assumed to be localized on the atoms is then included for the first time in melting studies. The interplay between magnetic and cohesive interactions is shown to give rise to interesting effects such as cluster volume contraction and sharper melting, as well as a magnetic transition at low temperature. Application to Ni, Co, and Fe clusters is discussed.

### I. INTRODUCTION

Microclusters have been subject recently to extensive studies, both theoretically and experimentally. Many aspects and properties have been investigated by various methods from different points of view. The interest in microclusters is no doubt due to potential applications in microdevices. For a recent bibliography, the reader is referred to Ref. 1.

As for the atomic structure of a microcluster containing  $10-10^3$  atoms where the number of surface atoms is larger than or comparable to that of inside atoms, the following questions have been raised. Is it like a solid in which atoms are oscillating around their respective equilibrium positions or is it like a liquid in which atoms diffuse on the surface and/or inside of the system? Or, is it like a solid whose structure is fluctuating among different configurations? Recently, temporal changes of the atomic structure of a gold cluster of  $10^2$  atoms on a  $\text{SiO}_2$  surface have been observed by using a high-resolution electron microscope.<sup>2</sup> The result shows that the structure is fluctuating among different configurations, in particular those of a cuboctahedron, an icosahedron, and a liquid droplet. It has been discussed<sup>2</sup> that such a structural fluctuation may be induced by charge fluctuations. However, more recent experiments have shown that the structural change is due to the internal temperature.<sup>3</sup>

In this paper, we investigate the melting transition in microclusters made of transition-metal atoms. The melting transition was studied many years ago by molecular dynamics<sup>4</sup> (MD) and Monte Carlo (MC) simulations.<sup>5,6</sup> More recently, progress has been made by Berry and co-workers,<sup>7-10</sup> and Quirke<sup>11</sup> among others.<sup>1</sup> These works focused on clusters of rare-gas atoms using the well-known Lennard-Jones (LJ) potential. In particular, from their MD results, Berry and co-workers have suggested that solid- and liquidlike phases coexist between what they called the freezing temperature and the melting temperature, first for 13-atom clusters<sup>8,9</sup> and later for other

sizes.<sup>10</sup> Sawada<sup>12</sup> has found that in transition-metal clusters of six and seven atoms, the structure oscillates between the ground state and the metastable states in the temperature range between the solid and the liquid phases. Quirke has reported, on the other hand, that while the melting transition is continuous for a 13-atom cluster in spherical cavities, it is of first order for 201- and 209-atom clusters, using MC simulation.<sup>11</sup>

The purpose of this work is twofold: (i) By using a potential appropriate for transition metals, we investigate the melting behavior of small clusters of sizes from 7 to 17 atoms and compare the results to those obtained with LJ potential; (ii) next, by including *for the first time* in melting studies a long-range magnetic interaction to simulate real magnetic clusters such as Ni, Co, and Fe, we study the magnetic ordering and the interplay between melting and magnetic phase transitions.

Interest in magnetic clusters has been found in different domains. Recently, clusters of Co have been experimentally studied in connection with fractal dimension<sup>13</sup> where the role of magnetic coupling *between* clusters has been shown. This has been found in agreement with numerical simulations<sup>14</sup> assuming magnetic dipolar interaction between clusters. Quantum tunneling of magnetization in small ferromagnetic particles has also been investigated.<sup>15</sup> In the present work, magnetic moments are assumed to be localized on atoms in a cluster and interact with each other. This model is somewhat justified by a recent microscopic calculation of the electronic structure of small transition-metal clusters by Fujima and Yamaguchi.<sup>16</sup> Magnetic ordering found in the present work for small clusters justifies the assumption of cluster magnetic moments used in the above-mentioned studies.<sup>13-15</sup>

For our purposes, extensive MC simulations have been performed on the Supercomputer SX-2 at the NEC Corporation through a highly vectorized program. The results in the case without magnetic interaction show that for very small clusters, our potential [see (1) below] yields many features similar to those obtained from the LJ po-

tential with the melting temperature oscillating with increasing cluster size. These clusters can be classified into two groups corresponding to stable and metastable structures characterized by different melting behaviors. When magnetic interactions are included, several interesting aspects are found. In particular, magnetic interactions make the melting transition sharper and give rise to a cluster volume contraction similar to the well-known magnetostriction in bulk materials. Among the most striking features is the existence of a magnetic ordering at finite temperatures for very small clusters, which would not be possible without the interaction between magnetic and cohesive forces.

Section II is devoted to the description of the model and MC technique. Results without and with magnetic interaction are shown and discussed in Sec. III. Concluding remarks are given in Sec. IV.

## II. MODEL AND MONTE CARLO TECHNIQUE

We use the following model potential which has been employed to study properties of transition-metal surfaces<sup>17</sup> and clusters,<sup>18,19,12</sup>

$$V(r_i) = U \left\{ A \sum_j \exp[-p(r_{ij} - r_0)] - \left[ \sum_j \exp[-2q(r_{ij} - r_0)] \right]^{1/2} \right\}, \quad (1)$$

where  $r_{ij}$  is the distance between the two atoms at  $r_i$  and  $r_j$ ,  $r_0$  is the nearest-neighbor distance of the bulk crystal (fcc), and  $U$ ,  $A$ ,  $p$ , and  $q$  are parameters. The sums are performed over all atoms in the cluster. The value of  $A$  is determined by minimizing the cohesive energy of the bulk crystal with nearest-neighbor distance  $r_0$ , while the values of  $U$ ,  $p$ , and  $q$  are determined in such a way that the bulk cohesive energy and the bulk modulus calculated by using (1) and the experimental value of  $r_0$  are in good agreement with the corresponding experimental results. The values  $p=9/r_0$  and  $q=3/r_0$  are found to be appropriate for transition metals.<sup>17</sup> Using  $A=0.101035$ , the bulk cohesive energy is given by  $E_{\text{bulk}}=1.17674U$ . In the following, we shall use  $r_0$  and  $U$  as the units of distance and energy, respectively. In the potential (1), many-body interactions are included through the square root of the second sum. The square-root form of the interaction sum has also been used in transition-metal studies by Finnis and coworkers.<sup>20</sup> For a detailed discussion of (1), the reader is referred to Refs. 17–19.

For the first time in melting studies, we include a long-range magnetic interaction between spins associated with the atoms. The magnetic Hamiltonian is given by

$$H = - \sum_{i,j} J(r_{ij}) S_i S_j, \quad (2)$$

where the spin  $S_i$  at the  $i$ th atom is assumed for simplicity to be Ising-type with values  $\pm 1$ , and the distance-dependent exchange integral  $J(r_{ij})$  between the  $i$ th and  $j$ th spins is given by the following simple form:

$$J(r_{ij}) = J_0 \exp(-\alpha r_{ij}), \quad (3)$$

where  $J_0$  and  $\alpha$  are parameters chosen in such a way as to fit the bulk Curie temperature. For bulk Ni, Co, and Fe, the Curie temperatures  $T_C$  are 631, 1404, and 1043 K, and the melting temperatures  $T_m$  are 1726, 1766, and 1808 K, respectively, which correspond to 0.0388, 0.0400, and 0.04236 in our units of energy. For the respective materials, the cohesive energies are 102.7, 102.2, and 99.5 kcal/mol or 4.455, 4.433, and 4.316 eV per atom. From the mean-field approximation  $T_C = 2S(S+1)zJ_e/3k_B$  where  $S$  is the spin magnitude,  $z$  the number of nearest neighbors (NN), and  $k_B$  the Boltzmann constant, one obtains the values of  $0.3398 \times 10^{-2}$ ,  $0.4032 \times 10^{-2}$ , and  $0.2808 \times 10^{-2}$  eV for the exchange integral  $J_e$  between NN in Ni, Co, and Fe, respectively ( $S=1$  and  $z=12$  for Ni,  $S=\frac{3}{2}$  and  $z=12$  for Co, and  $S=2$  and  $z=8$  for Fe have been used). These values by the mean field are certainly not accurate; in reality they may be several times larger because it is known that the factor in the expression of  $T_C$  is overestimated. We caution that apart from the inaccuracy of mean field, these values may be different in clusters due to possible changes of electronic structures. However, for the purpose of the present work, the order of magnitude suffices. The ratios between magnetic and cohesive energies at equilibrium are then 0.07%, 0.1%, and 0.07%, approximately for Ni, Co, and Fe.

One has only one condition to satisfy, i.e., the ratio  $[J(r_0)]/[V(r_0)]$ , but two parameters  $J_0$  and  $\alpha$  to choose. Note that positive and negative  $J_0$  corresponds to ferromagnetic and antiferromagnetic interactions, respectively. We limit ourselves to the former case because long-range antiferromagnetic interactions will cause *frustration*<sup>21</sup> whose effects are very interesting but complicated for the present study; this case is left for future investigations. Choosing arbitrarily  $J_0$  to be 5 and  $\alpha$  equal to 6.9, the ratio between magnetic and cohesive energies at equilibrium is approximately equal to 0.5%. In our simulations, we take this ratio which is larger than those calculated for Ni, Co, and Fe above to recompensate the underestimated values of  $J_e$  by the mean field already discussed. Figure 1 shows  $V$  and  $J(r_{ij})$  as functions of distance for two atoms. Note that one can have another choice of  $J_0$  and  $\alpha$  keeping unchanged the ratio between magnetic and cohesive energies at equilibrium. In this case, the new values of  $J_0$  and  $\alpha$  will affect the curvature of  $J(r_{ij})$  in Fig. 1. It is, however, believed that general aspects of the results shown later in this paper will not be altered. We will return to this point later.

Extensive MC simulations have been carried out using (1) with and without the magnetic interaction (2) for comparison. The MC method used can be briefly described by the following steps: (i) generating a random configuration of atom positions and spin orientations; (ii) equilibrating the system at a fixed temperature  $T$  by single-atom moving and spin-flipping over  $2 \times 10^5$  MC steps *per atom* (the updating procedure is detailed below); and (iii) averaging physical quantities over the next  $2 \times 10^5$  MC steps per atom. Many independent runs (up to 10) have been performed for each size to ensure the reproducibility of the results shown later in this paper,

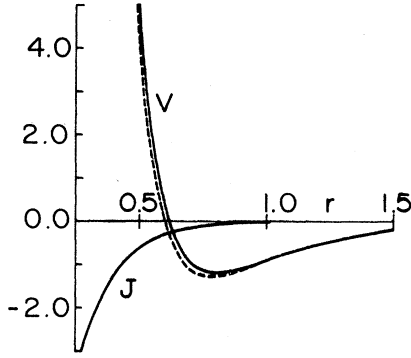


FIG. 1. Cohesive potential  $V$  and exchange integral  $J$  vs interatomic distance  $r$  for two-atom cluster. The total potential  $V+J$  is shown by the dashed line. The parameters for  $J$  are  $J_0=5$  and  $\alpha=6.9$ . For clarity,  $J$  was multiplied by 4 in the figure so that the dashed line is seen.

especially the most stable structures in the solid phase.

The updating procedure is done as follows: (i) choosing a random atom and calculating its total energy  $E_1$  (magnetic and cohesive interactions); (ii) moving it to a random nearby position and taking a random new spin orientation, then calculating its new total energy  $E_2$ ; and (iii) if  $E_2$  is lower than  $E_1$  then the new state is accepted, otherwise it is accepted only with a probability  $\exp[-\beta(E_2-E_1)]$  where  $\beta=(k_B T)^{-1}$ . Note that it is the total energy that matters so magnetic and cohesive interactions are taken into account simultaneously. The following physical quantities are averaged: internal energy per atom  $E$ , magnetization per spin  $M$ , mean bond length  $L$ , bond-length distribution  $P(r)$ , specific heat per atom  $C$ , magnetic susceptibility per spin  $\chi$  and bond length fluctuations  $\Delta$ . The last three quantities and  $L$  are defined as

$$C = (\langle E^2 \rangle - \langle E \rangle^2) / (Nk_B T^2), \quad (4)$$

$$\chi = (\langle M^2 \rangle - \langle M \rangle^2) / (NT), \quad (5)$$

$$\Delta = 2 \sum_{i,j} (\langle r_{ij}^2 \rangle - \langle r_{ij} \rangle^2)^{1/2} / \langle r_{ij} \rangle / N(N-1), \quad (6)$$

$$L = 2 \sum_{i,j} \langle r_{ij} \rangle / N(N-1), \quad (7)$$

where  $N$  is the number of atoms in the cluster and  $\langle \dots \rangle$  means averaged value taken during the total simulation time after equilibration. In the following  $k_B$  is set to be 1.

The cluster sizes studied in this paper are from  $N=7$  to 17. Larger sizes are subject to future investigations.

### III. RESULTS AND DISCUSSION

In this section results without and with the magnetic interaction are shown and compared.

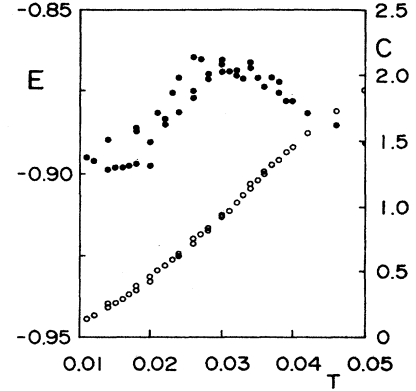


FIG. 2. Internal energy  $E$  (open circles, left scale) and specific heat  $C$  (solid circles, right scale) vs temperature  $T$  for  $N=13$  without magnetic interaction.

#### A. Nonmagnetic case

##### 1. Melting behavior

Figure 2 shows in internal energy per atom  $E$  and specific heat  $C$  calculated from energy fluctuations (4) as functions of  $T$  in the case of  $N=13$  without magnetic interaction. The peak of  $C$  corresponds to the change of curvature of  $E$  at  $T \approx 0.03$ . It is rather broad and shows fluctuations especially on the low-temperature side. The averaged bond length  $L$  and bond length fluctuations  $\Delta$  versus  $T$  are displayed in Fig. 3 for the same case.  $L$  undergoes a gradual change of slope starting from the temperature where  $\Delta$  begins to jump ( $T \approx 0.02$ ) and ending at the temperature where  $\Delta$  saturates. Note that the latter temperature, denoted as  $T_m$  hereafter, corresponds to the peak of  $C$ .

The large temperature region between the beginning and the end of the jump of  $\Delta$  has also been found in the case of LJ potential by Berry and coworkers,<sup>9,10</sup> who in-

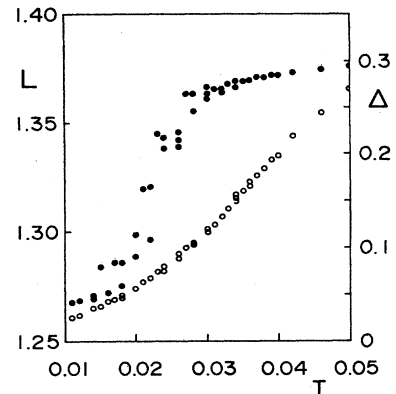


FIG. 3. Mean bond length  $L$  (open circles, left scale) and bondlength fluctuations  $\Delta$  (solid circles, right scale) vs  $T$  for  $N=13$  without magnetic interaction.

terpreted this as the coexistence region of solid and liquid phases. The word "coexistence" should not be understood as solid and liquid phases coexisting at the same time, as it is usually understood at first-order transition point. Rather, it has been shown that the cluster (except  $N=8$  and 14) goes back and forth to and from two different energy levels (bimodal energy distribution) during a characteristic time.<sup>10</sup> For us, the physical picture is rather clear: the cluster in the so-called coexistence region goes from one minimum free-energy valley to another by climbing up some rather flat energy barrier during a characteristic time; the energy values in the valley and up on the barrier where the system stays for some time give rise to the bimodal distribution. The frequent changes from one minimum to another are certainly due to the fact that there is a large number of nearly degenerate states in small clusters. This situation is somewhat similar to spin glasses where the spin-glass transition is found, in general, at a temperature lower than that at the peak of  $C$  (see K. H. Fisher in Ref. 21). Note that Quirke<sup>11</sup> has used with some caution the peak position of  $C$  to identify the melting temperature from solid to liquid phase for clusters in cavity. At this stage, it is worthwhile to note that while the physical picture in the coexistence region is clear, the definition of two temperatures for freezing and melting<sup>10</sup> cannot be viewed as the existence of two distinct transitions because of the lack of further evidence such as two peaks in  $C$ , etc. To define two transitions, one needs some other physical quantities (order parameters) which characterize different phases.

Figure 4 shows the distribution of interatomic distance  $P(r)$  for  $N=13$  at  $T=0.11$  and 0.020. The peaks correspond to first-, second-, and third-neighbor distances. For higher temperatures, the first peak is still seen but the second and third ones collapse into a single broad peak.

## 2. Structures at finite temperatures

Among the sizes from 7 to 17, the structure for  $N=13$  is the most stable one (icosahedron). The stability is quite

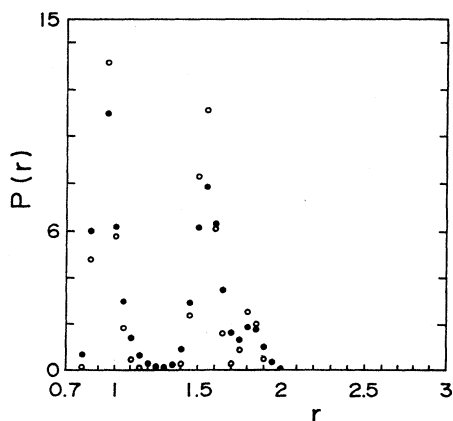


FIG. 4. Bond length distribution  $P(r)$  vs  $r$  for  $N=13$  at  $T=0.011$  (open circles) and  $T=0.02$  (solid circles).

different for other sizes. From the viewpoint of melting behavior, it is convenient to classify these structures into two categories.

(i) The stable structures: They are characterized by a change of curvature of  $E$  in the plot  $E$  versus  $T$  in the transition region; this is also seen by a maximum of the specific heat  $C$  calculated by energy fluctuations.

(ii) The metastable structures: They show neither a change of curvature of  $E$  nor a peak in  $C$ .

These two categories show, however, a jump in  $\Delta$ . The first category includes the following sizes:  $N=13, 12, 7,$  and  $11$ , in order of decreasing stability judged from the peak intensity of  $C$ . The second category includes all other sizes. As an example of this category, we show in Fig. 5 the case of  $N=17$ .

The stable structures at finite  $T$  in the solid phase have some simple pentagonal symmetries rather easy to recognize. For example, the structure of  $N=7$  in the solid phase is a pentagonal bipyramid consisting of a ring of five atoms with one atom on the top and another at the bottom. The structure of  $N=11$  at low  $T$  consists of two rings of five atoms plus one atom on the top [Fig. 6(a)], the 13-atom cluster has the well-known icosahedron structure, and the structure of  $N=12$  is that of  $N=13$  minus one on the top. The metastable structures, on the other hand, have either no particular symmetries, a mixing of pentagonal and hexagonal symmetries [see Figs. 6(b) and 6(c) for  $N=14$  and  $N=17$ , respectively], or other symmetries such as trisquare pyramid for  $N=9$  [Fig. 6(d)], hexagonal for  $N=15$  [Fig. 6(e)] and  $N=16$  [Fig. 6(f)], Werfelmeier's tetragonal hemihedron<sup>22</sup> for  $N=8$  and pentagonal bipyramid plus three for  $N=10$  [Fig. 6(h)].

Note that the structures for the metastable category are not the most stable ones in the ground state (GS) given by Hoare and Pal<sup>22</sup> in the case of LJ potential. It seems, therefore, interesting to study the GS with the potential (1) for different  $N$  and to compare with the LJ case and to the structures found at finite  $T$  shown above. There are two foreseen possibilities: (i) If the GS determined with (1) are the same as in the LJ case, then the

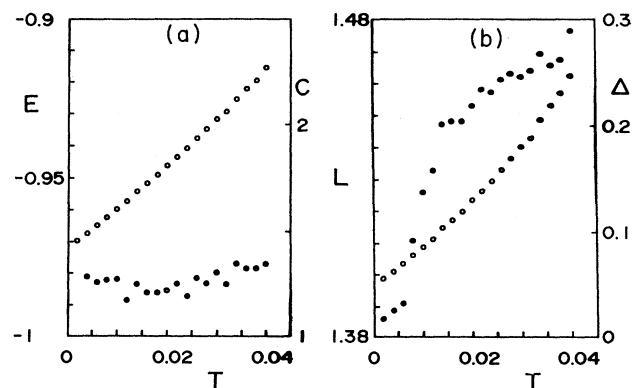


FIG. 5.  $N=17$  without magnetic interaction: (a)  $E$  and  $C$  vs  $T$  (open and solid circles, respectively); (b)  $L$  and  $\Delta$  vs  $T$  (open and solid circles, respectively).

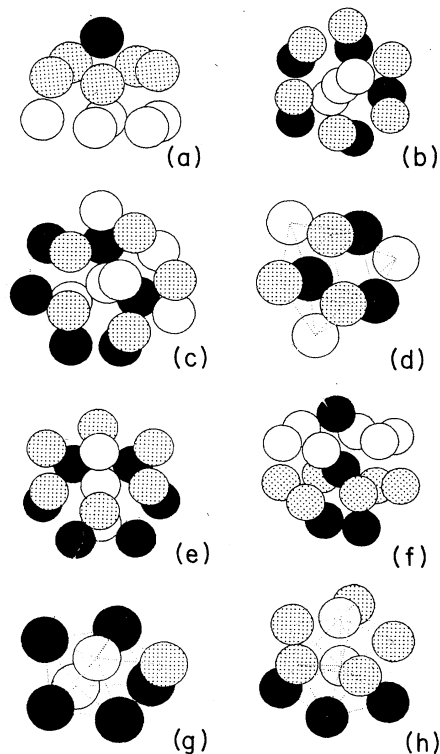


FIG. 6. Structures at finite  $T$  ( $T=0.002$ ). Particular symmetries are highlighted by sphere colors: (a)  $N=11$ , (b)  $N=14$ , (c)  $N=17$ , (d)  $N=9$ , (e)  $N=15$ , (f)  $N=16$ , (g)  $N=8$  (shaded circle and solid circle behind it have equivalent positions with respect to the four solid circles), and (h)  $N=10$  (structure of  $N=7$  plus three solid circles).

structures found here may be the most stable structures selected by the entropy effect (maximum density of states) though they do not have the lowest energies in the GS; (ii) if the GS determined with (1) are the same as those observed here at finite  $T$ , then the difference with the LJ case is very interesting. The study of GS structures is, therefore, necessary. This requires extensive work and is left for future investigations.

As expected, there is a close relation between the structure symmetry and the melting behavior. The second category has, in general, a very low melting temperature. In the absence of a proper definition of the melting point, let us show in Fig. 7 as a function of cluster size  $N$  the temperatures at the limits of the coexistence region defined at the lower and upper limits of the jump in  $\Delta$ . Whenever it exists, the temperature at the maximum  $C$ ,  $T_m$ , corresponds more or less to the temperature at the upper limit. The results of the LJ potential taken from Beck *et al.*<sup>10</sup> are also shown for comparison (only temperatures at which  $\Delta$  rises sharply are reported for the clarity of the figure). For small sizes, our potential and the LJ one give the same behavior, but there is a small deviation for larger sizes (from  $N=14$ ). This may be due

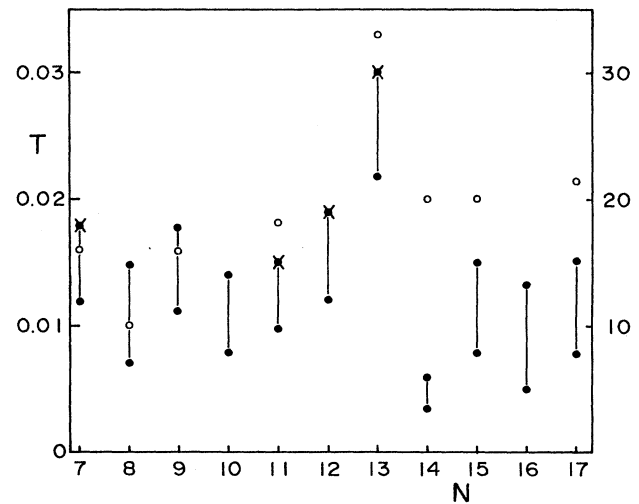


FIG. 7. Characteristic temperatures vs  $N$  in the absence of magnetic interaction. Vertical bars limited by solid circles are limits of the jump of  $\Delta$  and crosses indicate peak temperatures of  $C$  (only four sizes, see text). Results with LJ potential from Ref. 10 by open circles with right scale (in degrees Kelvin) are shown for comparison.

to the many-body effect of our potential when  $N$  gets large enough.

## B. Magnetic case

### 1. Melting behavior

We show now the effects of the magnetic interaction. For the sizes studied here, the magnetic interaction gives somewhat similar effects. For a size in the stable category ( $N=7, 11, 12, 13$ ), one observes that the scattering of points in the nonmagnetic case is strongly suppressed and the peak of  $C$  is sharper. But the effect of magnetic interaction is markedly felt in the metastable structures with the appearance of a change of curvature in  $E$  corresponding to the maximum  $C$ , which does not exist in the nonmagnetic case. Figure 8 shows  $E$  and  $C$  versus  $T$  in the typical cases with  $N=13$  and  $N=17$ .

It is now interesting to ask the question of why magnetic interaction makes the melting transition sharper. A partial answer is found when one looks at the total potential shown in Fig. 1. The magnetic interaction enhances the anharmonicity around the potential minimum. This suppresses a number of metastable states, i.e., reduces structural fluctuations and therefore makes the melting transition sharper.

$L$  and  $\Delta$ , on the other hand, show behavior similar to the nonmagnetic case, i.e., a large coexistence region (Fig. 9). However, the striking feature observed here is that  $L$  is smaller in the presence of magnetic interactions at a given temperature. For example, from  $T=0.011$  to  $T=0.017$ ,  $L$  varies on a straight line from 1.253 to 1.261 in the magnetic case, compared to values of  $L$  from 1.261

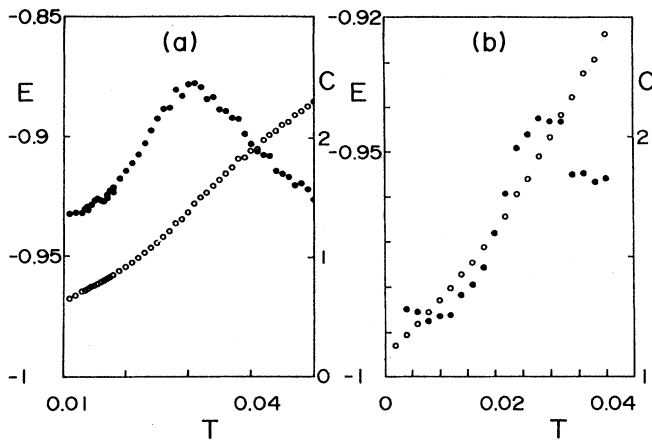


FIG. 8.  $E$  (open circles, left scale) and  $C$  (solid circles, right scale) vs  $T$  with magnetic interaction for  $N=13$  (a) and  $N=17$  (b).

to 1.269 in the nonmagnetic case for the same range of temperature. The contraction of the cluster volume due to magnetic interaction is similar to the so-called magnetostriction effect observed in bulk magnetic materials. It is noted that the structure remains that of the corresponding nonmagnetic case.

## 2. Magnetic transition

One of the most interesting results in the magnetic case is the existence of ferromagnetic ordering at low temperatures. Figure 10 shows magnetization  $M$  and magnetic susceptibility  $\chi$  versus  $T$  for  $N=7$  and 13. The magnetic transition takes place below the melting at  $T_C \simeq 0.010$  and  $\simeq 0.018$  for  $N=7$  and 13, respectively. The jump of  $\chi$  at the magnetic transition from the low-temperature side is delta-functionlike. On the high temperature side,

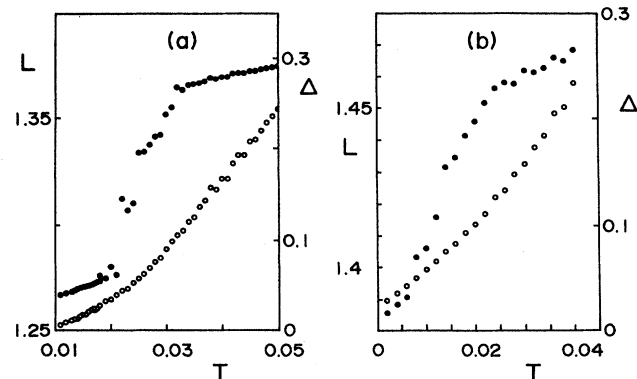


FIG. 9.  $L$  (open circles, left scale) and  $\Delta$  (solid circles, right scale) vs  $T$  with magnetic interaction for  $N=13$  (a) and  $N=17$  (b).

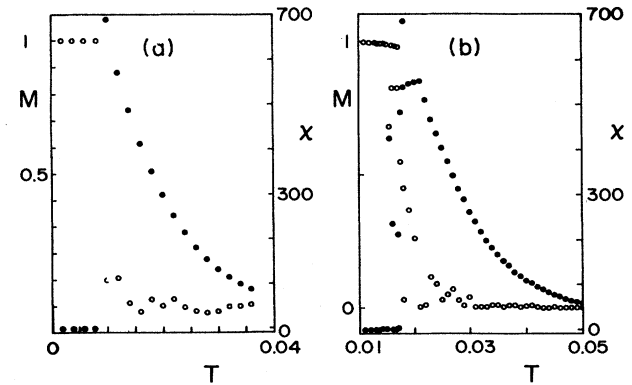


FIG. 10. Magnetization  $M$  (open circles, left scale) and magnetic susceptibility  $\chi$  (solid circles, right scale) vs  $T$  for  $N=7$  (a) and  $N=13$  (b).

it has a very smooth behavior. The same behavior is also seen for the other sizes including the metastable category defined above (see Fig. 11 for  $N=15$  and 17). Note that no peak in  $C$  is observed at the magnetic transition. This is due to the fact that the magnetic energy is very small compared to the cohesive energy, so the magnetic energy fluctuations at  $T_C$  are not pronounced enough to be seen.

The existence of magnetic ordering for clusters as small as  $N=7$  is a consequence of the interplay between magnetic and cohesive interactions. For small clusters of sizes studied here, magnetic ordering at finite  $T$  cannot exist, at least from MC simulations, if the cohesive interaction (1) is not included. The magnetic ordering found here can therefore be called *phonon-assisted magnetic ordering*.

We show in Fig. 12 the magnetic transition temperature  $T_C$  and  $T_m$  as function of  $N$ . A few remarks are in order: (a)  $T_m$  is slightly increased compared to the nonmagnetic case (Fig. 7) but with similar tendency; (b) a

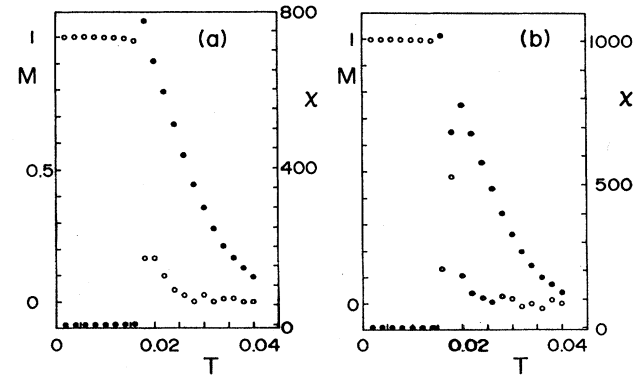


FIG. 11. Magnetization  $M$  (open circles, left scale) and magnetic susceptibility  $\chi$  (solid circles, right scale) vs  $T$  for  $N=15$  (a) and  $N=17$  (b).

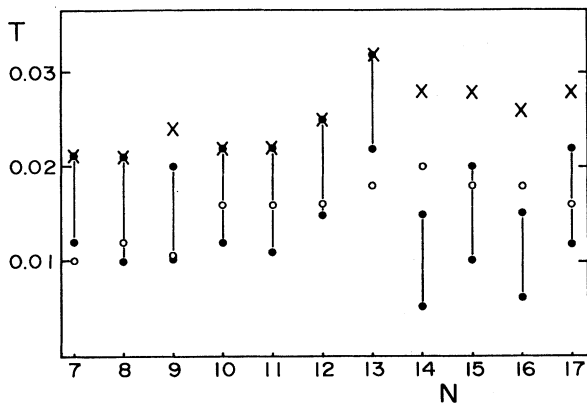


FIG. 12. Characteristic temperatures vs  $N$  in the presence of magnetic interaction. Vertical bars limited by solid circles are limits of the jump of  $\Delta$ , crosses indicate peak temperatures of  $C$ , and open circles are Curie temperatures.

maximum in  $C$  is observed for all sizes and in the metastable category (except  $N=8$ ); the maximum of  $C$  is found above the upper limit of the jump in  $\Delta$ ; (c)  $T_C$  in all cases is below  $T_m$ , but in some sizes, it is above the upper limit ( $N=14$ , for example) or below the lower limit of the jump in  $\Delta$  ( $N=13$ , for instance).

Now, in view of the smooth behavior of  $\chi$  above the magnetic transition, it is interesting to calculate the critical exponent  $\gamma$  associated with this transition for clusters. Using the relation

$$\chi = R(T - T_C)^{-\gamma}, \quad (8)$$

where  $R$  is a constant, the critical exponent  $\gamma$  has been calculated for different  $N$  studied in this work. As an example, a log-log plot of (8) for the case  $N=13$  is shown in Fig. 13, using  $T_C=0.018$ . From the slope of the straight line drawn by a mean least-squares fit, one obtains

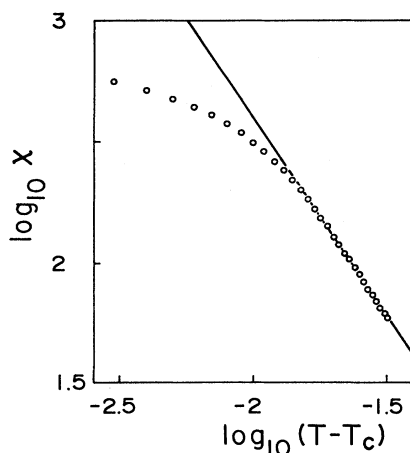


FIG. 13. Log-log plot of Eq. (8) for  $N=13$ . The slope of the straight line obtained from a least-squares fit yields exponent  $\gamma=1.620$ .

$\gamma=1.62\pm 0.10$ . The error was calculated from the error on the value of  $T_C$  which is estimated at  $\pm 0.001$ . It is noted that the deviation from the straight line when  $T \rightarrow T_C$  is expected: Due to the finite-size effect,  $\chi$  does not diverge at  $T_C$  following (8). Now, it is interesting to notice that the value of  $\gamma$  obtained here is between the values for Ising spin systems in two and three dimensions, which are 1.75 and  $\approx 1.25$ , respectively.<sup>23</sup> We emphasize, however, that these values have been calculated for the case of short-range interactions in the absence of cohesive interactions.

We have also calculated  $\gamma$  for other cluster sizes. The results show that  $\gamma$  oscillates between the bi- and tridimensional values: For example,  $\gamma=1.52, 1.70, 1.33, 1.56$ , and  $1.70$  for  $N=7, 9, 11, 15$ , and  $17$ , respectively (error for all cases is  $\pm 0.1$ ). The oscillatory behavior may be closely related to that of  $T_m$  shown in Fig. 12 due to different structural stabilities.

#### IV. CONCLUDING REMARKS

To conclude, let us emphasize the following points.

(a) When only cohesive interaction (1) is taken into account (nonmagnetic case), the melting behavior depends on the cluster size. It is convenient to distinguish two categories, stable and less-stable structures, characterized by different melting behaviors. The former, including  $N=7, 11, 12$ , and  $13$ , has a maximum in  $C$  while the latter has not. The melting is recognized in this case by a jump in  $\Delta$  which occurs, in general, at very low  $T$ .

(b) Melting is preceded by a large region of temperature where strong fluctuations are observed. Similar features have been found in the LJ case and were interpreted as coexistence of solid and liquid phases.<sup>10</sup>

(c) A long-range magnetic interaction has been included for the first time in melting studies. Its effects are remarkably seen: sharper melting transition especially in the less stable category where a maximum in  $C$  appears, and cluster volume contraction (magnetostriction). However, the magnetic interaction leaves the cluster structure unchanged.

(d) One of the most striking results is the existence of magnetic ordering at finite  $T$  for clusters as small as  $N=7$ . The magnetic transition occurring below the melting is characterized by the loss of magnetization and an anomaly in the magnetic susceptibility. The associated "critical" exponent  $\gamma$  is found to depend on the cluster size. For  $N=7$  to  $17$ ,  $\gamma$  has values between those of Ising spin systems in two and three dimensions.

The magnetic ordering at finite  $T$  for such small clusters is possible only in the presence of the cohesive potential. In this sense, one can say that the magnetic and cohesive interactions help each other to eliminate fluctuations and therefore enhance the stability of the cluster.

As the last remarks, let us mention that the results have been shown for  $\alpha=6.9$  and  $J_0=5$ , which reproduces approximately the order of magnitude of the ratio between magnetic and cohesive energies at equilibrium in bulk transition metals such as Ni, Co, and Fe. Another choice of these parameters for the same ratio will change the curvature of  $J(r_{ij})$  in Fig. 1. Stronger curvature will

likely enhance the volume contraction and, furthermore, suppress structure fluctuations, making melting transition sharper. Besides, the simple magnetic model used here can be improved in future work to represent real transition-metal clusters. Finally, it is hoped that this paper will stimulate more experiments and theoretical investigations on melting in magnetic clusters.

#### ACKNOWLEDGMENTS

One of us (H.T.D.) is grateful to Fundamental Research Laboratories of the NEC Corporation for its generous support and hospitality. We wish to thank Dr. S. Ohnishi for his interest in this work and helpful discussions.

\*On leave from Laboratoire de Magnétisme des Surfaces, Université Paris 7, 75251 Paris CEDEX 05, France.

<sup>1</sup>*Microclusters*, edited by S. Sugano, Y. Nishina, and S. Ohnishi (Springer-Verlag, Berlin, 1987).

<sup>2</sup>S. Iijima and T. Ichihashi, *Phys. Rev. Lett.* **56**, 616 (1986); S. Iijima, in Ref. 1, p. 186.

<sup>3</sup>K. Takayanagi (private communication); *Z. Phys. D* (to be published).

<sup>4</sup>C. L. Briant and J. J. Burton, *J. Chem. Phys.* **63**, 2045 (1975).

<sup>5</sup>J. B. Kaelberer and R. D. Eppers, *J. Chem. Phys.* **66**, 3233 (1977); **66**, 5112 (1977).

<sup>6</sup>V. V. Nauchitel and A. J. Pertsin, *Mol. Phys.* **40**, 1341 (1980).

<sup>7</sup>R. S. Berry, J. Jellinek, and G. Natanson, *Chem. Phys. Lett.* **107**, 227 (1984); *Phys. Rev. A* **30**, 919 (1984).

<sup>8</sup>J. Jellinek, T. L. Beck, and R. S. Berry, *J. Chem. Phys.* **84**, 2783 (1986).

<sup>9</sup>H. Davis, J. Jellinek, and R. S. Berry, *J. Chem. Phys.* **86**, 6456 (1987).

<sup>10</sup>T. L. Beck, J. Jellinek, and R. S. Berry, *J. Chem. Phys.* **87**, 545 (1987); T. L. Beck and R. S. Berry, *ibid.* **88**, 3910 (1988).

<sup>11</sup>N. Quirke, *Mol. Simulation* **1**, 249 (1988).

<sup>12</sup>S. Sawada, in Ref. 1, p. 211; S. Sawada and S. Sugano, *Z. Phys. D* (to be published).

<sup>13</sup>G. A. Niklasson *et al.*, *Phys. Rev. Lett.* **60**, 1735 (1988).

<sup>14</sup>P. M. Mors *et al.*, *J. Phys. A* **20**, L975 (1987).

<sup>15</sup>E. M. Chudnowsky and L. Gunther, *Phys. Rev. Lett.* **60**, 661 (1988).

<sup>16</sup>N. Fujima and T. Yamaguchi, *J. Phys. Soc. Jpn.* (to be published).

<sup>17</sup>R. P. Gupta, *Phys. Rev. B* **23**, 6265 (1981).

<sup>18</sup>M. B. Gordon, F. Cyrot-Lackmann, and M. C. Desjonqueres, *Surf. Sci.* **80**, 159 (1979).

<sup>19</sup>D. Tomanek, S. Mukherjee, and K. H. Bennemann, *Phys. Rev. B* **28**, 665 (1983).

<sup>20</sup>M. W. Finnis and J. E. Sinclair, *Philos. Mag. A* **50**, 45 (1984); G. J. Ackland and M. W. Finnis, *ibid.* **54**, 301 (1986).

<sup>21</sup>For frustrated systems, see R. Liebmann, *Statistical Mechanics of Periodic Frustrated Ising Systems*, Vol. 251 of *Lecture Notes in Physics* (Springer-Verlag, Berlin, 1986). For spin glasses, see, for instance, *Proceedings of the Heidelberg Colloquium on Spin Glasses* (Springer, Berlin, 1983); also K. H. Fisher, *Phys. Status Solidi B* **116**, 357 (1983).

<sup>22</sup>M. R. Hoare and P. Pal, *Adv. Phys.* **20**, 161 (1971); *J. Cryst. Growth* **17**, 77 (1972).

<sup>23</sup>See, e.g., R. B. Stinchcombe, in *Phase Transitions and Critical Phenomena*, edited by C. Domb and J. L. Lebowitz (Academic, New York, 1983), Vol. 7, p. 176.